STM JOURNALS

Journal of
Water Pollution &
Purification Research

ISSN: 2394-7306
Volume 12, Issue 3, 2025
September–December
DOI (Journal): 10.37591/JoWPPR

https://journals.stmjournals.com/jowppr

Research JoWPPR

Green Fabrication of Glutaraldehyde-Crosslinked Chitosan/PVA Biocomposite for Heavy Metal Removal from Wastewater

Siddharth Anand[1,*], Rahul V. Anand[2]

Abstract

Chitosan (CS) and Polyvinyl alcohol (PVA) are polymers that possess biodegradable, biocompatible, and non-toxic properties, making them suitable for wastewater treatment applications. The primary objective of this research is to chemically modify chitosan in a novel manner to enhance its ability to remove hexavalent chromium Cr(VI) from aqueous solutions. In this study, a composite material was synthesized by crosslinking PVA and CS with glutaraldehyde (GA), resulting in the formation of a CS/PVA/GA composite to eliminate Cr(VI) through batch adsorption experiments effectively. The synthesized adsorbents were characterized using Field Emission Scanning Electron Microscopy with Energy Dispersive X-ray Spectroscopy (FESEM-EDS), X-ray Diffraction (XRD), Brunauer Emmett Teller (BET), and Fourier Transform Infrared Spectroscopy (FTIR) to examine surface morphology, structural properties, porosity, and functional groups. The effects of various parameters such as initial Cr(VI) concentration, pH, adsorbent dosage and contact time were systematically studied to optimize adsorption performance. The adsorption kinetics followed the pseudo-second-order model, indicating that chemisorption is the rate-limiting step. Among the tested isotherm models, the Freundlich isotherm model provided the best fit to the equilibrium data, suggesting heterogeneous surface adsorption. The CS/PVA/GA composite demonstrated a maximum adsorption capacity of 98.9 mg/g, which is significantly higher compared to unmodified chitosan or other conventional adsorbents. Furthermore, the material exhibited excellent reusability; even after three adsorption-desorption cycles, the composite maintained a desorption efficiency of 73%, showing minimal loss in performance. These results confirm the potential of CS/PVA/GA as a sustainable, cost-effective, and efficient adsorbent for the removal of toxic Cr(VI) ions from contaminated water systems.

Keywords: Cr(VI), chitosan, polyvinyl alcohol, glutaraldehyde, adsorption

***Author for Correspondence**
Siddharth Anand
E-mail: sid.v.anand1994@gmail.com

[1]Assistant Professor, Department of Humanities and Applied Sciences, Echelon Institute of Technology, Faridabad, India
[2]Assistant Professor, Department of Information Technology, Jagannath International Management School (Vasant Kunj), New Delhi, India

Received Date: August 05, 2025
Accepted Date: August 20, 2025
Published Date: August 30, 2025

Citation: Siddharth Anand, Rahul V. Anand. Green Fabrication of Glutaraldehyde-Crosslinked Chitosan/PVA Biocomposite for Heavy Metal Removal from Wastewater. Journal of Water Pollution & Purification Research. 2025; 12(3): 59–83p.

INTRODUCTION

The contamination of water resources by heavy metals has emerged as a serious global issue due to their toxicity, non-biodegradability, and tendency to bioaccumulate in living organisms. Chromium, in particular, is one of the most widespread and hazardous heavy metals found in industrial effluents, originating from activities such as electroplating, leather tanning, metal finishing, textile processing, and stainless steel manufacturing [1]. It contaminates both surface and groundwater, posing significant risks to environmental and human health. In the environment, chromium predominantly exists in two oxidation states:

trivalent chromium (Cr(III)) and hexavalent chromium (Cr(VI)). Cr(III) is an essential micronutrient involved in glucose metabolism, whereas Cr(VI) is highly toxic and carcinogenic, classified as a Group "A" human carcinogen by the United States Environmental Protection Agency (USEPA) and the World Health Organization (WHO) [2, 3]. Due to its high solubility and weak interactions with inorganic surfaces, Cr(VI) is more mobile in aqueous environments and can easily penetrate biological membranes. Chronic exposure to Cr(VI) has been linked to a wide range of adverse health effects, including liver and kidney damage, respiratory problems, skin disorders, immune system suppression, genetic mutations, and cancer [4]. As a result, the WHO recommends that the concentration of Cr(VI) in drinking water should not exceed 0.05 mg/l.

Various treatment methods have been employed for the removal of Cr(VI) from contaminated water, including chemical precipitation, ion exchange, membrane filtration, electrochemical treatment, and adsorption. Among these, adsorption has gained considerable attention due to its simplicity, cost-effectiveness, high removal efficiency, and potential for adsorbent regeneration and reuse [5]. However, the efficiency of adsorption greatly depends on the nature and characteristics of the adsorbent material.

In recent years, natural biopolymers have been increasingly explored for their potential as low-cost and eco-friendly adsorbents. Chitosan, a polysaccharide obtained by the deacetylation of chitin, exhibits excellent chelation capabilities owing to the presence of amino and hydroxyl functional groups. It is also biodegradable, non-toxic, and abundant, making it an ideal adsorbent for heavy metal adsorption [6]. Nevertheless, native chitosan has certain limitations, including high crystallinity, low mechanical strength, and poor stability in acidic conditions, which restrict its practical application [7]. To address these issues, various chemical and physical modifications have been developed, such as crosslinking, grafting, and blending with other polymers.

Polyvinyl alcohol (PVA), a synthetic polymer known for its hydrophilicity, biocompatibility, chemical resistance, and mechanical robustness, has been widely used to enhance the properties of chitosan-based adsorbents [8]. When chitosan is blended with PVA and subsequently crosslinked using agents such as glutaraldehyde, the resulting composite exhibits improved structural integrity and adsorption capacity [9]. These chitosan-PVA (CS/PVA) composites have shown promise in water treatment applications, particularly for the removal of heavy metals like Cr(VI).

Given the environmental and health hazards posed by Cr(VI), this study aims to synthesize and evaluate crosslinked CS/PVA composites for the adsorption of Cr(VI) from aqueous solutions. The prepared materials were characterized using Field Emission Scanning Electron Microscopy with Energy Dispersive X-ray Spectroscopy (FESEM-EDS) to analyze surface morphology, Fourier Transform Infrared Spectroscopy (FTIR) to identify the functional groups, X-ray Diffraction (XRD) to examine structural properties and Brunauer Emmett Teller (BET) to analyze porosity. The influence of various operational parameters such as initial Cr(VI) concentration, pH, adsorbent dosage and contact time was systematically investigated. Additionally, adsorption kinetics and isotherm parameters were evaluated to understand the mechanism and equilibrium behavior.

This research aims to contribute to the development of sustainable and efficient biosorbents for the removal of hexavalent chromium from wastewater, offering an environmentally friendly alternative to conventional treatment methods.

MATERIALS AND METHODS

Materials

First, Chitosan ($C_6H_{11}NO_4$) with a degree of deacetylation greater than 80% was procured from Merck, India. Potassium dichromate ($K_2Cr_2O_7$) was obtained from Qualigens, India. Polyvinyl alcohol (PVA) (C_2H_4O), acetic acid (CH_3COOH), sodium hydroxide (NaOH), glutaraldehyde ($C_5H_8O_2$), 1,5-diphenylcarbazide ($C_{13}H_{14}N_4O$), and acetone (C_3H_6O) were also obtained from standard commercial

sources. All reagents used were of analytical grade. Solutions were prepared using distilled water throughout the study.

Synthesis of CS/PVA

Chitosan solution was prepared by dissolving 4 g of chitosan powder in a 4% v/v acetic acid solution, followed by continuous stirring at room temperature for 24 h. Separately, a polyvinyl alcohol (PVA) solution was prepared by dissolving 4 g of PVA in 36 ml of deionized water and heating under reflux at 90°C for 3 h. The two prepared solutions were then combined and stirred magnetically at 150 rpm for 3 h to obtain a homogeneous mixture. The resulting solution was allowed to stand undisturbed for 2 h to remove entrapped air bubbles [10].

Subsequently, the composite solution was introduced dropwise into a 0.2 M NaOH solution using a 2 ml syringe needle, leading to the formation of the CS/PVA composite beads. The beads were further immersed in 0.2 M NaOH for 2 h to neutralize residual acetic acid. After the neutralization step, the composites were filtered using Whatman filter paper and washed thoroughly with distilled water until the filtrate was free of alkali [11].

Synthesis of CS/PVA/GA

The washed CS/PVA composite was suspended in a solution containing 99 ml of ethanol and 1 ml of glutaraldehyde, and the mixture was stirred at 70°C for 5 h to facilitate crosslinking between chitosan and glutaraldehyde [12]. Following the crosslinking reaction, the composite was filtered and washed thoroughly with ethanol to remove any unreacted glutaraldehyde. The material was then rinsed with deionized water until a neutral pH was achieved. Finally, the CS/PVA/GA composite was dried at room temperature. The synthesis pathway for the CS/PVA/GA composite is illustrated in Figure 1.

Instrumentation and characterization

All absorption measurements were conducted at room temperature using a double-beam UV-visible spectrophotometer (Spectro UV-Vis Double Beam 3500, India). The pH of the solutions was measured using a digital pH meter (Kings Lab, India). Separation of the supernatant and adsorbent was performed using Whatman filter paper.

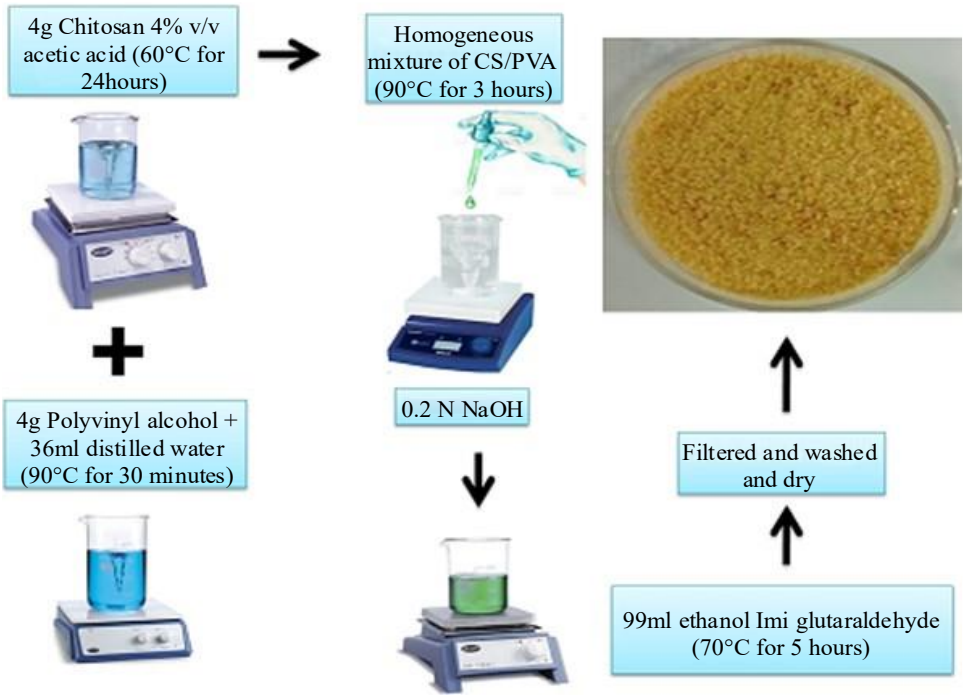

Figure 1. Synthesis of modified chitosan composite using PVA and GA.

The structural, morphological, and surface properties of the adsorbent before and after Cr(VI) adsorption were analyzed using various techniques. The surface morphology was examined via Field Emission Scanning Electron Microscopy (FESEM) using an FEI NOVA NANO FESEM 450 instrument. SEM images were obtained at a magnification of 1000× under an accelerating voltage of 5 kV. The elemental composition of the adsorbents was determined through Energy Dispersive X-ray Analysis (EDAX).

The crystallinity of the samples was investigated using X-ray Diffraction (XRD) analysis (PANalytical X'Pert Powder) with CuKα radiation (λ=1.5406 Å). Diffraction patterns were recorded in the 2θ range of 10–90°, using a step size of 0.02° and a counting time of 0.5 sec.

Fourier Transform Infrared (FTIR) spectroscopy (Shimadzu 8400S) was used to identify the functional groups present in the samples. Spectra were recorded in the range of 400–4000 cm^{-1} using the KBr pellet technique with a mid-IR DTGS detector.

The specific surface area, pore volume, and pore size distribution of the adsorbent were analyzed using Brunauer-Emmett-Teller (BET) surface area analysis, conducted on a NOVA TOUCH LX2 (Quantachrome Instruments, USA) using nitrogen adsorption-desorption isotherms.

Adsorption experiments

A synthetic Cr(VI) solution with a concentration of 100 mg/l was prepared using potassium dichromate ($K_2Cr_2O_7$). The concentration of Cr(VI) in the solution was determined using the 1,5-diphenylcarbazide method. For this, the diphenylcarbazide reagent was prepared by dissolving 250 mg of 1,5-diphenylcarbazide in 50 ml of acetone and stored in a brown bottle to prevent photodegradation.

For the analysis, 10 ml of the Cr(VI) solution was taken in a test tube, followed by the addition of 5 drops of orthophosphoric acid to maintain an acidic medium. Subsequently, 2 ml of the diphenylcarbazide reagent was added, and the mixture was shaken for 2 min. The absorbance was then measured at 540 nm using a UV-Vis spectrophotometer [13].

Batch adsorption experiments were conducted in 250 ml conical flasks, each containing 30 ml of the 100 mg/l Cr(VI) solution. A 1 g portion of the synthesized CS/PVA/GA composite was added to each flask. The flasks were then placed on a magnetic stirrer at 150 rpm under ambient conditions. After the predetermined contact time, the adsorbent was separated from the solution using Whatman filter paper, and the residual Cr(VI) concentration in the filtrate was measured spectrophotometrically [14].

The adsorption capacity (q_e) and the Cr(VI) removal efficiency (%) were calculated using Eqs. (1) and (2), respectively.

$$q_e = \frac{v(C_0 - C_e)}{m} \quad (1)$$

$$\text{Cr (VI) removal efficiency (\%)} = \frac{C_0 - C_e}{C_0} \times 100 \quad (2)$$

Where, q_e is the maximum adsorption capacity (mg/g), C_0 is the initial Cr(VI) concentration (mg/l), Ce is the equilibrium (final) Cr(VI) concentration (mg/l), V is the volume of the solution (l), and m is the mass of the CS/PVA/GA composite used (g) [15].

RESULTS AND DISCUSSION

Adsorbent Characterization

FESEM

The surface morphology of pure chitosan (CS), the CS/PVA/GA composite, and the CS/PVA/GA composite after Cr(VI) adsorption (CS/PVA/GA/Cr) was examined using Scanning Electron Microscopy (SEM), as illustrated in Figure 2(a) and Figure 2(b). The SEM image of pure CS displays

a smooth and regular surface, indicative of its unmodified structure [16]. In contrast, the CS/PVA/GA composite exhibits a more structured morphology with well-aligned polymer chains, likely resulting from crosslinking interactions between chitosan and polyvinyl alcohol through functional groups such as $–NH_2$ and –OH (Table 1).

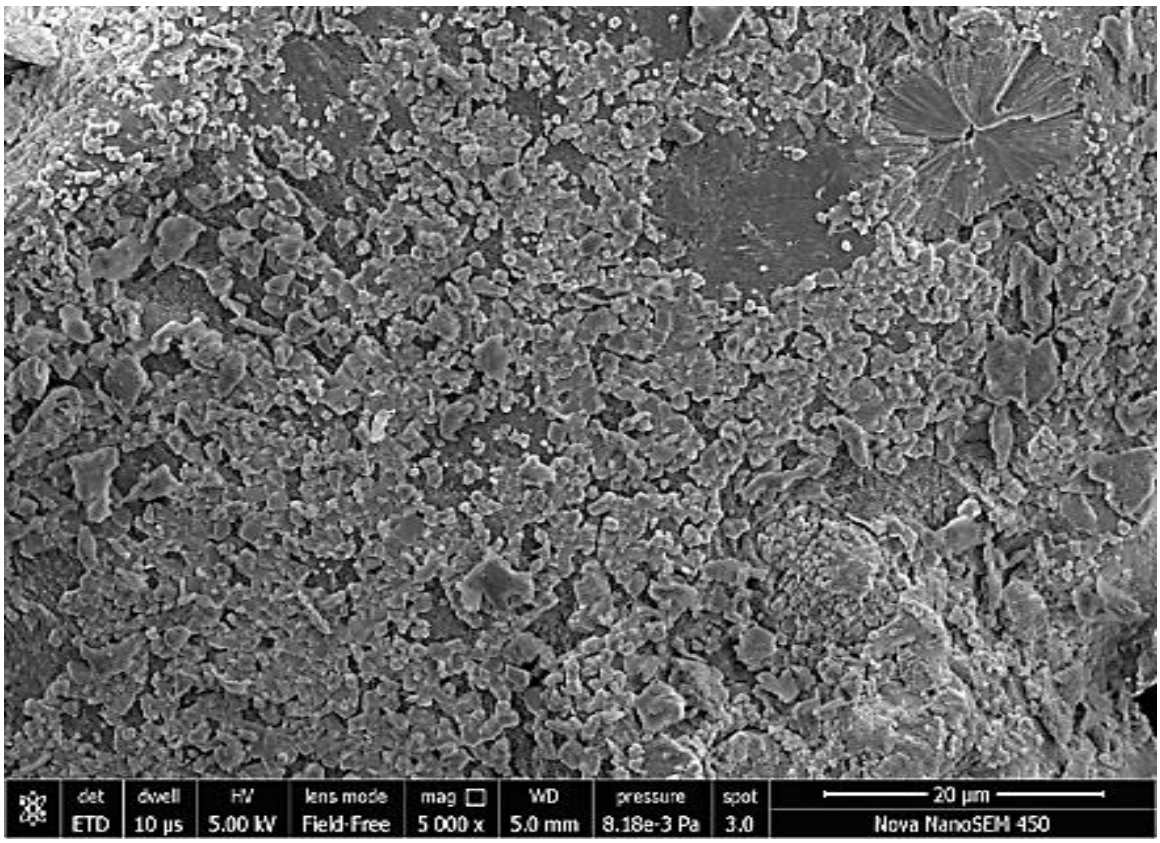

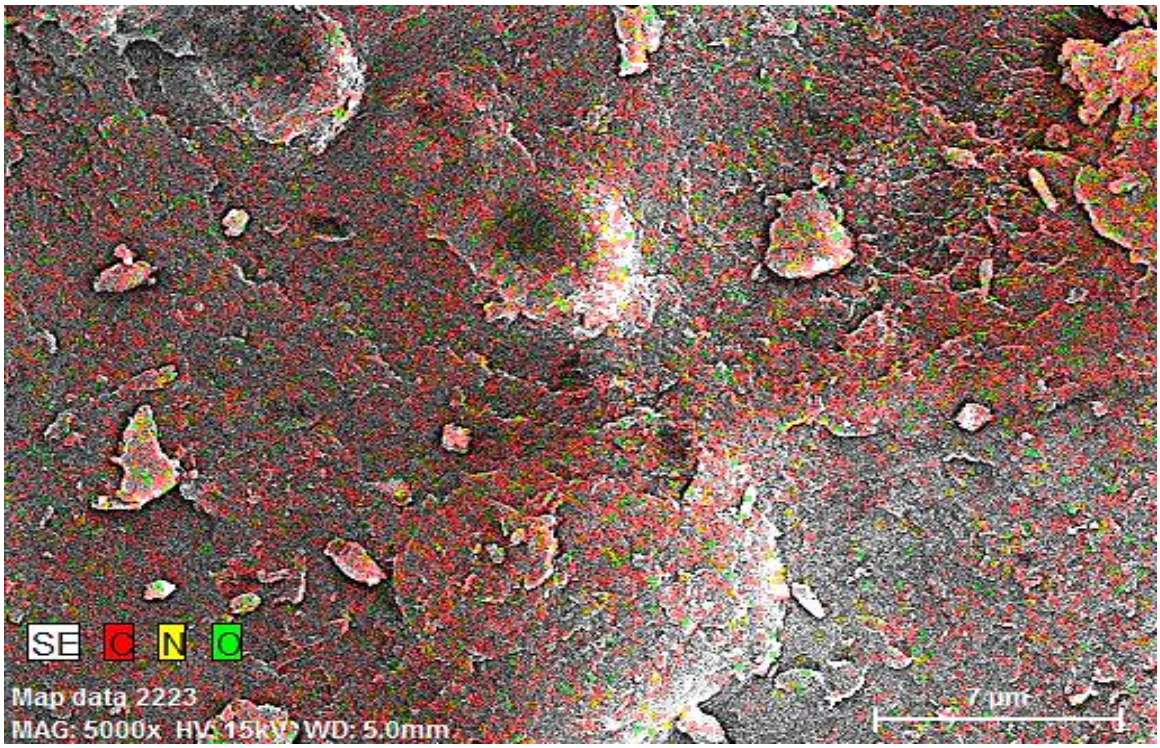

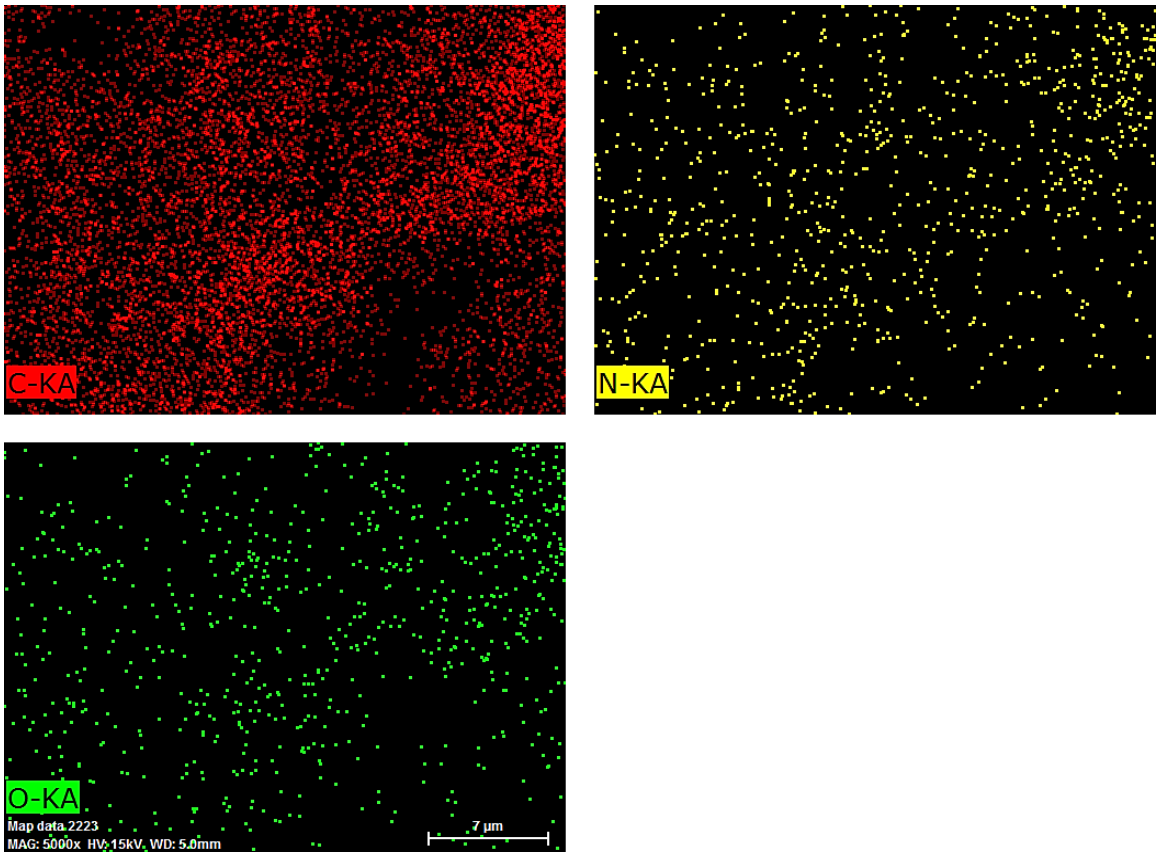

Figure 2(a). FESEM spectra and EDS mapping of commercial Chitosan.

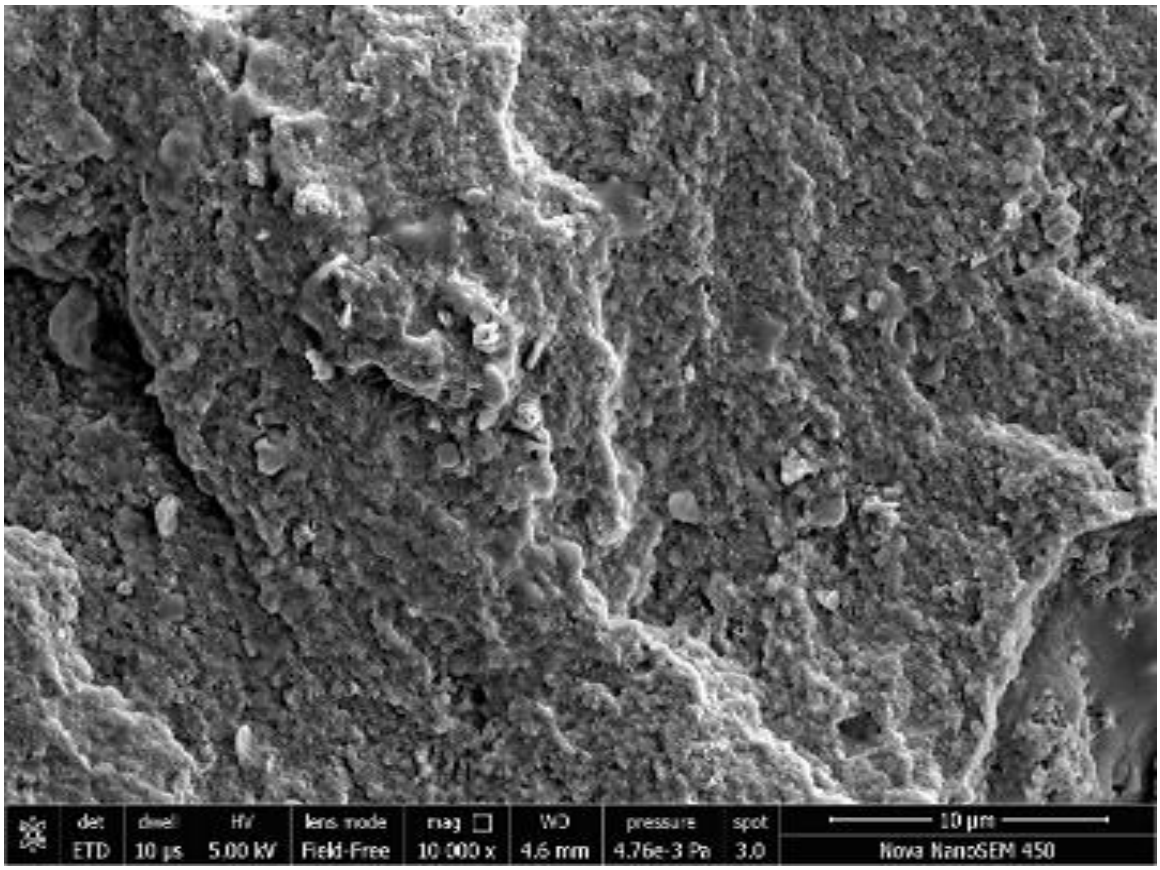

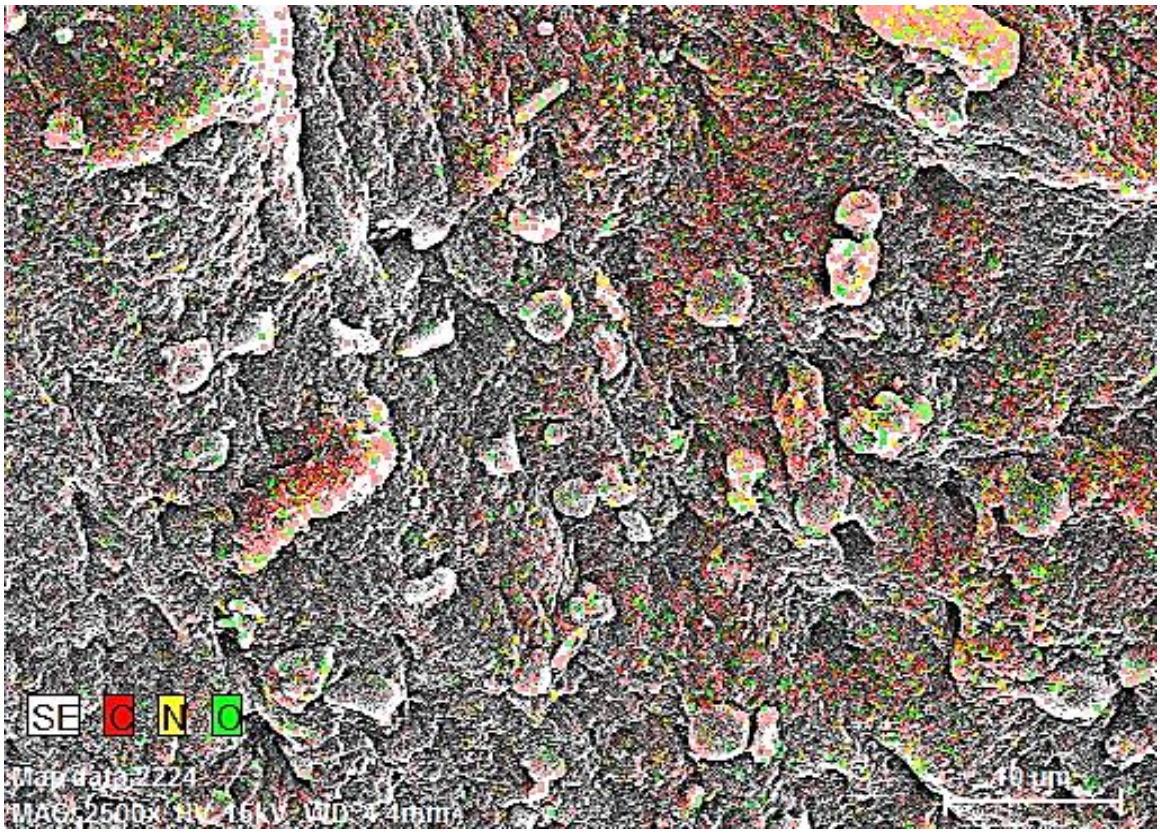

Figure 2(b). FESEM spectra and EDS mapping of synthesized CS/PVA/GA composite.

Table 1. EDS analysis of commercial Chitosan and Synthesized CS/PVA/GLA.

Elements	Commercial Chitosan (%)	CS/PVA/GLA composite	
		***Pre-Adsorption* (%)**	***Post-Adsorption* (%)**
C	61.58	64.48	61.50
N	27.19	19.73	21.22
O	11.23	15.78	17.28

After Cr(VI) adsorption, the SEM image of the CS/PVA/GA/Cr composite reveals a rough and heterogeneous surface texture, suggesting successful adsorption of Cr(VI) ions onto the composite surface. These morphological changes confirm the structural and surface alterations due to both crosslinking and adsorption process [17].

FTIR

FTIR analysis was conducted to investigate the molecular interactions and functional group changes during the formation of the CS/PVA/GA composite and its interaction with Cr(VI) ions. The FTIR spectra of CS, CS/PVA/GA, and CS/PVA/GA/Cr are presented in Figure 3.

In the FTIR spectrum of pure chitosan (CS), characteristic peaks were observed at 3429.30, 2878.67, and 1653.21 cm^{-1}, corresponding to –OH and $–NH_2$ stretching vibrations, –CH stretching, and amide 1 bands, respectively [18]. The peak at 1599.12 cm^{-1} is attributed to $–NH_2$ bending vibrations, while the peaks at 1380.36 and 1155.33 cm^{-1} correspond to C–N stretching and O-bridge stretching, respectively. Additionally, peaks at 1030.95 and 1071.83 cm^{-1} indicate primary and secondary –C–OH stretching vibrations [19].

Upon the formation of the CS/PVA/GA composite, notable spectral shifts were observed. The broad absorption band at 3429.30 cm^{-1}, corresponding to –OH and $–NH_2$ stretching vibrations, shifted slightly

to 3427.73 cm^{-1}, indicating intermolecular hydrogen bonding. The free amino group band at 1599.12 cm^{-1} disappeared and was replaced by a new band at 1637.30 cm^{-1}, attributed to overlapping C=O stretching of PVA and N–H bending of CS. This shift suggests the involvement of amino groups in crosslinking with glutaraldehyde [20]. Furthermore, the primary and secondary –C–OH stretching band at 1071.95 cm^{-1} in CS shifted to 1028.01 cm^{-1} in the CS/PVA/GA composite, confirming the formation of hydrogen bonds and chemical interactions among $–NH_2$ and –OH groups.

After Cr(VI) adsorption, additional spectral shifts were observed. The broad –OH/$–NH_2$ stretching band shifted to 3435.32 cm^{-1}, while the amide band moved to 1631.65 cm^{-1} and the C–O stretching band appeared at 1113.10 cm^{-1} [11]. These changes confirm that Cr(VI) adsorption primarily occurs through interactions with the $–NH_2$ and –OH functional groups of the CS/PVA/GA composite [21].

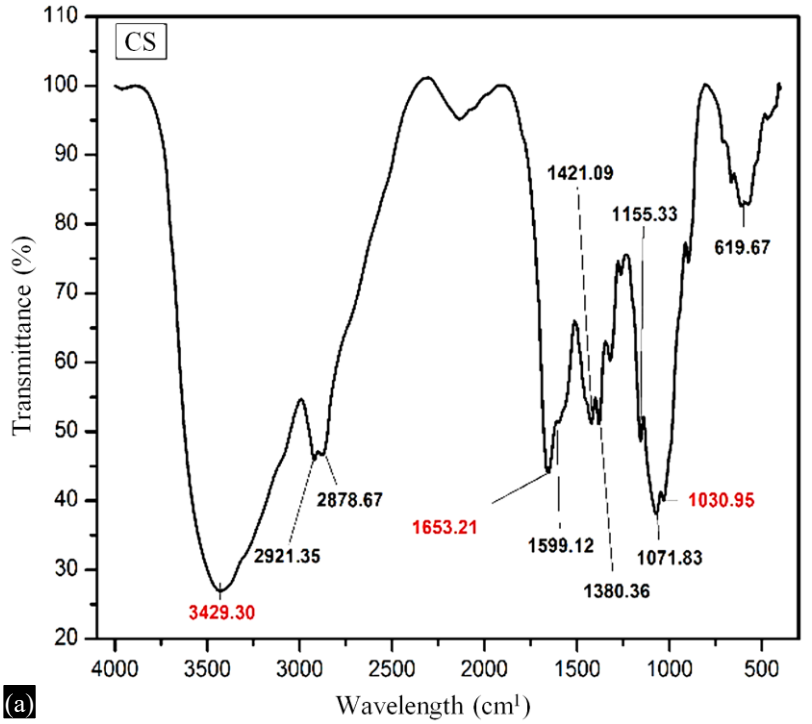

(a)

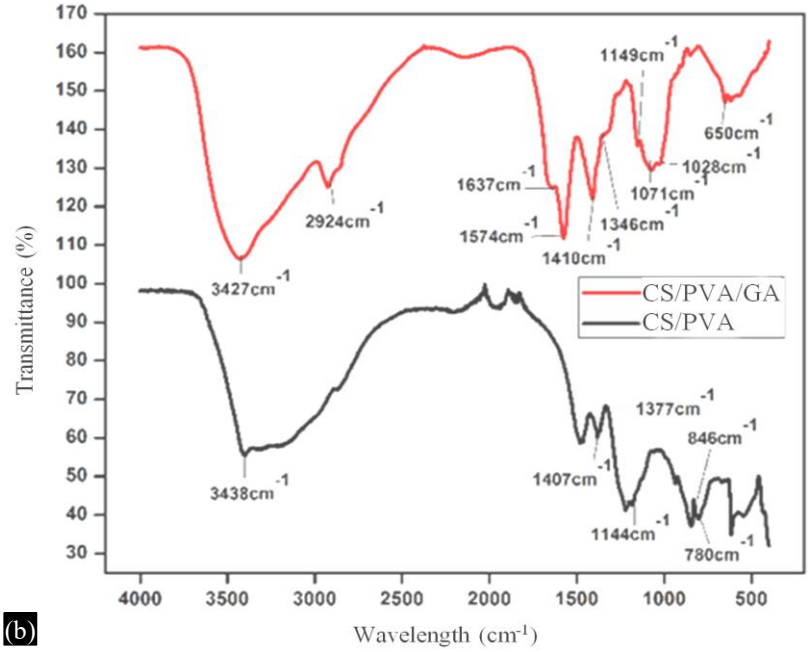

(b)

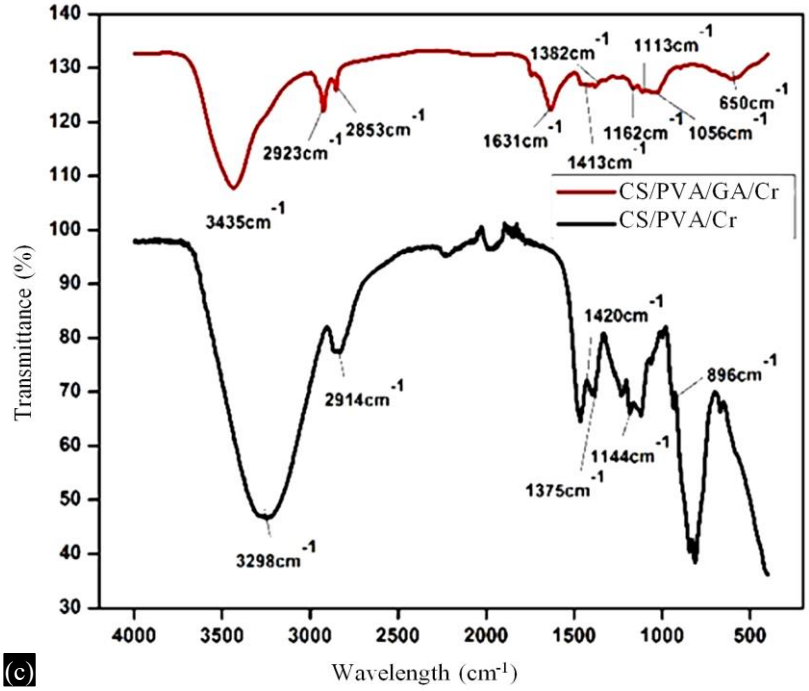

(c)

Figure 3. (a–c) The FTIR spectra of commercial chitosan and the synthesized CS/PVA and CS/PVA/GA composite before and after Cr(VI) adsorption.

XRD

The interaction between chitosan (CS) and polyvinyl alcohol (PVA) polymer chains significantly influences the physical properties of the resulting composite, including crystallinity, solubility, thermal and chemical stability, and ion exchange capacity [17]. Since crystallinity is closely associated with the mechanical properties of polymeric materials, X-ray diffraction (XRD) analysis was performed to evaluate the crystalline structure of CS, CS/PVA, and CS/PVA/GA composites before and after Cr(VI) adsorption. The results are presented in Figure 4.

XRD patterns were recorded over a 2θ range of 5 to 72.3°. According to existing literature, diffraction peaks around 2θ=27.1 and 34.1° are characteristic of chitosan and PVA, respectively [22]. In the current study, pure CS exhibited a prominent crystalline peak at 2θ = 26.7°, indicating its semi-crystalline nature. In the CS/PVA/GA composite, this peak shifted and intensified to 2θ=20.1°, suggesting that the crystallinity of CS was altered due to the chemical crosslinking reaction with glutaraldehyde [23]. This also reflects a partial disruption in the semi-crystalline structure of PVA, confirming the formation of a new crosslinked network between CS and PVA.

The observed changes can be attributed to strong hydrogen bonding interactions between the hydroxyl (–OH) groups of PVA and the amino (–NH_2) or hydroxyl (–OH) groups of chitosan, which disrupt the regular arrangement of polymer chains and decrease crystallinity [24]. After Cr(VI) adsorption, new diffraction peaks appeared at 2θ = 72.6°, indicating further reduction in crystallinity and confirming the adsorption of Cr(VI) onto the CS/PVA/GA composite matrix. These changes validate the successful chemical modification and functional performance of the composite in Cr(VI) removal.

BET

The specific surface area and pore size distribution (PSD) of the synthesized CS/PVA/GA composite were determined using nitrogen (N_2) adsorption-desorption isotherms [25]. The Brunauer Emmett Teller (BET) method was used to calculate the specific surface area, while the Barrett Joyner Halenda (BJH) method was used for pore size distribution analysis. The resulting isotherms and corresponding PSD plots are illustrated in Figure 5(a and b), respectively.

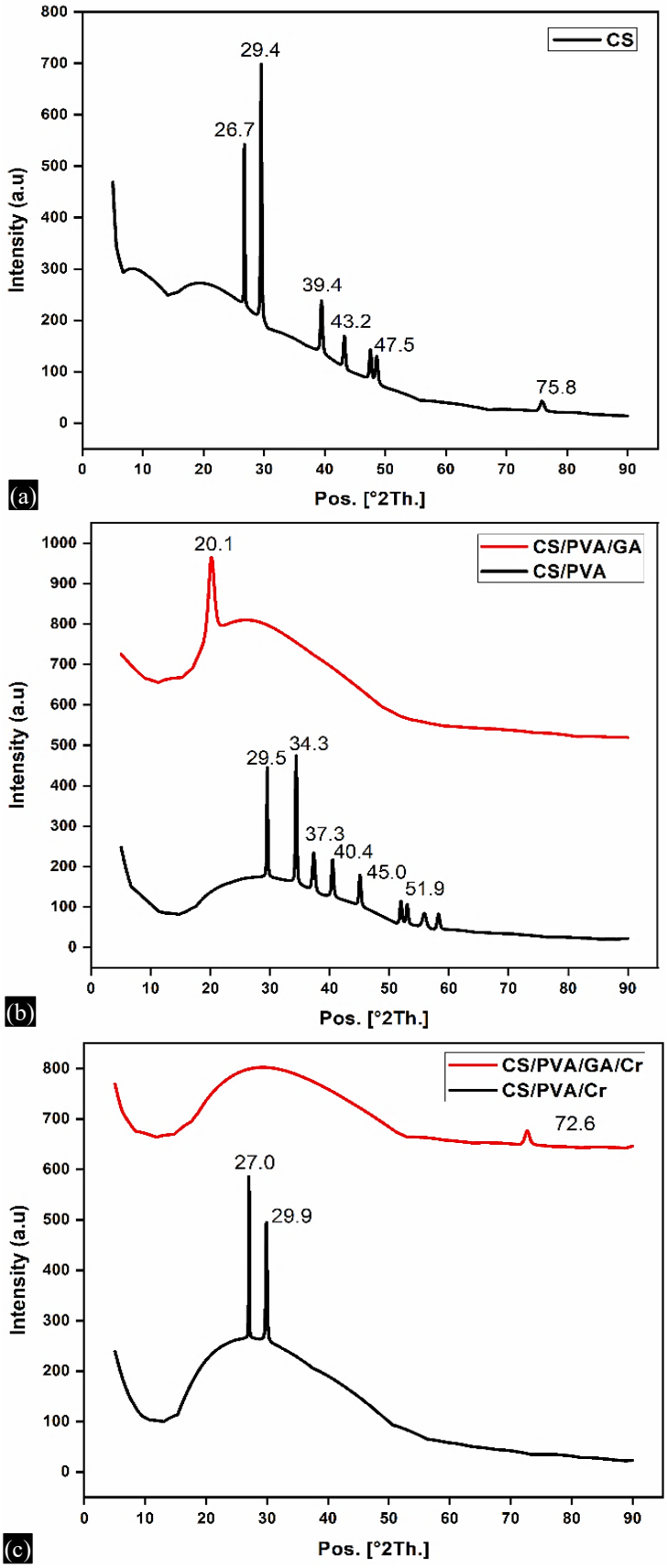

Figure 4. (a–c) The XRD spectra of commercial chitosan and the synthesized CS/PVA and CS/PVA/GA composite before and after Cr(VI) adsorption.

As shown in Figure 5(a), the composite exhibits a distinct hysteresis loop at relative pressures (P/P_0) above 0.7, characteristic of type IV isotherms, which is indicative of mesoporous structures [26]. Additionally, a noticeable increase in adsorption near $P/P_0 = 0.95–1.0$ suggests the presence of macropores, which likely arise due to the aggregation of polymer chains or entrapped air voids [27].

The pore size distribution in Figure 5(b) reveals that the majority of pores are larger than 3 nm, confirming the mesoporous nature of the composite. Furthermore, a minor peak observed at pore sizes slightly above 2 nm indicates the existence of micropores within the matrix, contributing to the overall porosity [28].

The chemical crosslinking and blending of CS with PVA resulted in the development of a well-structured porous network [29]. The BET surface area of the CS/PVA/GA composite was found to be 262.411 m^2/g, with a total pore volume of 0.604 cm^3/g, demonstrating the successful enhancement of the material's surface characteristics crucial for effective adsorption of heavy metal ions.

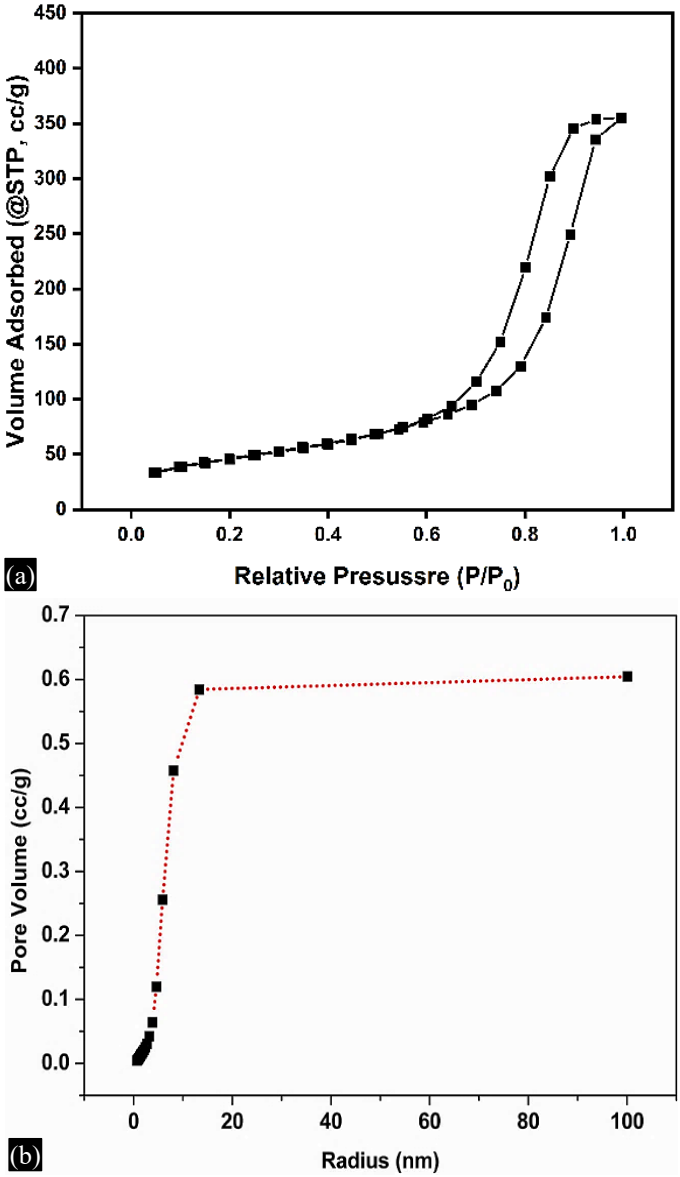

Figure 5. (a) N_2 adsorption-desorption curve of CS/PVA/GA composite.
(b) Pore size distributions of CS/PVA/GA composite.

Crosslinking of CS/PVA, with GA

The chemical stability of polymer composites can be significantly enhanced through chemical crosslinking, which reinforces the polymer network by forming covalent or ionic bonds, depending on the crosslinking agent employed. In the case of CS/PVA composites, ionic crosslinkers such as sodium tripolyphosphate (TPP) form electrostatic interactions that provide limited stability, particularly in acidic environments [30]. For instance, CS/PVA crosslinked with TPP tends to dissolve at pH 3, making it unsuitable for applications in low pH conditions.

In contrast, covalent crosslinkers like glutaraldehyde (GA) and epichlorohydrin establish robust, irreversible chemical bonds within the polymer matrix, enhancing structural integrity even under highly acidic conditions (pH 1) [31]. Among these, glutaraldehyde is widely recognized as a safer and more effective alternative to epichlorohydrin due to its lower toxicity, cost-effectiveness, and strong crosslinking efficiency [9].

Glutaraldehyde is a linear five-carbon dialdehyde that appears as a transparent, colorless, oily liquid with a pungent odor. It is highly soluble in water, alcohol, and organic solvents, which facilitates its use in polymer crosslinking [32]. The crosslinking mechanism of CS/PVA with glutaraldehyde is illustrated in Figure 6. GA reacts with the amine ($-NH_2$) groups of chitosan and hydroxyl (-OH) groups of PVA, forming stable covalent bonds that reinforce the polymer chains [33]. This cross-linking not only prevents the dissolution of the composite in strongly acidic media, such as hydrochloric acid but also improves its mechanical and chemical durability.

Moreover, the preservation and accessibility of amine functional groups in the polymer network are essential for effective adsorption performance [34]. The interaction between GA and CS/PVA enhances the availability of these groups, thereby increasing the adsorption capacity of the composite toward heavy metal ions such as Cr(VI) [11].

Batch Studies

Effect of pH

The pH of the solution plays a pivotal role in regulating both the surface charge of the adsorbent and the speciation of chromium ions in the solution, thereby directly influencing the adsorption capacity and removal efficiency [35].

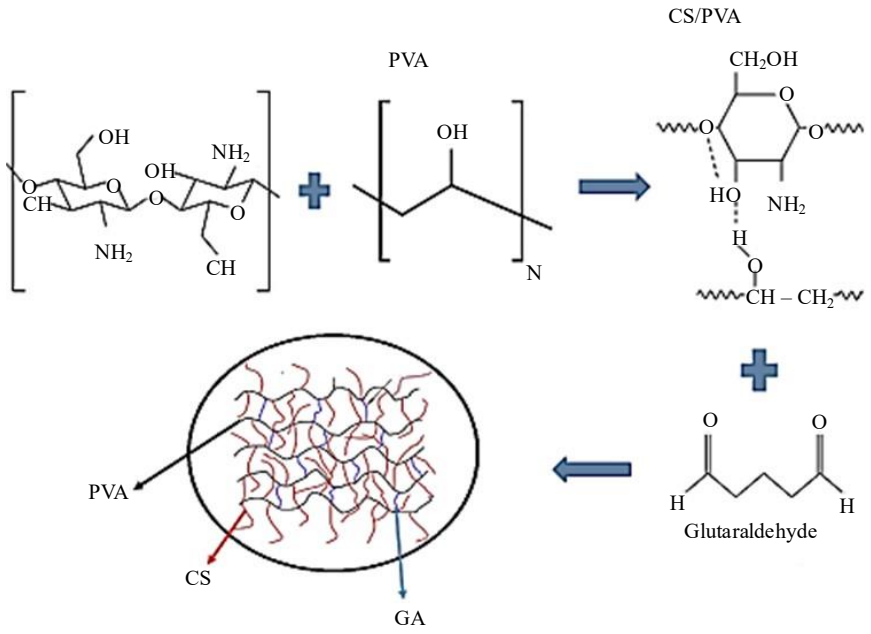

Figure 6. The crosslinking mechanism of CS/PVA with glutaraldehyde.

The literature widely reports that pH modulates electrostatic interactions between adsorbate and adsorbent surfaces, significantly affecting adsorption performance. In this study, batch adsorption experiments were performed to evaluate the adsorption efficiency of unmodified chitosan (CS), CS/PVA, and CS/PVA/GA composites across a pH range of 3 to 9. The experiments were conducted at 30°C using an initial Cr(VI) concentration of 50 mg/l, adsorbent dose of 1 g in 30 ml solution, stirring speed of 150 rpm and a contact time of 60 min. The resulting removal efficiencies are presented in Figure 7.

The results demonstrated a consistent trend: as pH increased from 3 to 9, the Cr(VI) removal efficiency decreased across all tested adsorbents. At pH 3, the removal efficiencies were highest, recorded as 98.8% for CS/PVA/GA, 44.3% for CS/PVA, and 18.6% for CS. This significant enhancement in removal efficiency at acidic pH is attributed to the surface protonation of functional groups (–NH_2 and –OH) on the composite, which imparts a net positive charge to the adsorbent surface. In acidic media, Cr(VI) primarily exists in the anionic form of hydrogen chromate ($HCrO_4^-$), which is electrostatically attracted to the positively charged surface of the adsorbent [36].

Moreover, the presence of excess H^+ ions in the solution at low pH conditions helps suppress surface negative charge and facilitates deeper penetration of $HCrO_4^-$ ions into the adsorbent matrix, thereby enhancing removal [37]. The observed results are consistent with previous findings, which reported similar behavior of chitosan-based materials under acidic conditions [38].

In contrast, under basic conditions (pH>7), Cr(VI) species such as CrO_4^{2-} and $Cr_2O_7^{2-}$ become dominant. Simultaneously, the adsorbent surface becomes less protonated, reducing the electrostatic attraction between negatively charged Cr(VI) species and the composite surface. Additionally, Cr(VI) reduction to Cr(III) is more favorable under basic conditions. Since Cr(III) is a cation, it experiences electrostatic repulsion from the increasingly negatively charged surface, further decreasing the adsorption efficiency. Therefore, the combined effect of chromate speciation and surface charge interactions explains the lower removal efficiencies observed at higher pH levels.

Effect of adsorbent dose

The influence of adsorbent dosage on the removal efficiency of Cr(VI) was investigated by varying the composite dosage from 0.25 to 1 g in 30 ml solution. The experiments were conducted at 30°C using an initial Cr(VI) concentration of 50 mg/l, pH of 3, stirring speed of 150 rpm and a contact time of 60 min. The results are depicted in Figure 8.

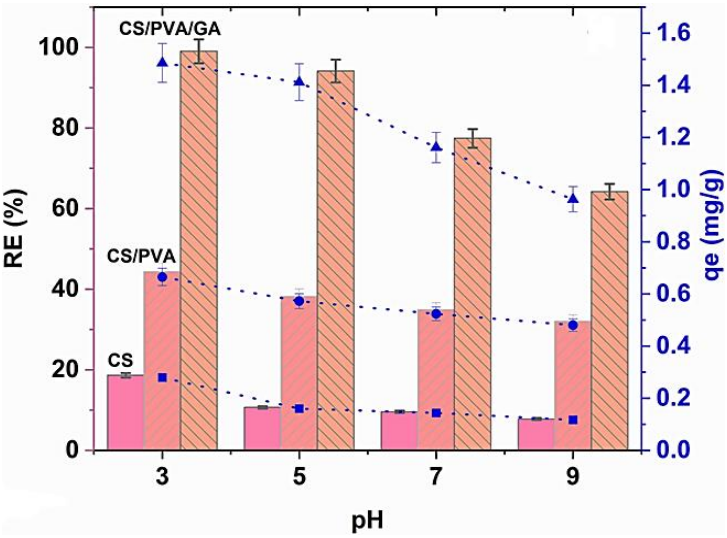

Figure 7. Effect of pH on the adsorption of Cr(VI) on CS, CS/PVA and CS/PVA/GA composite.

A consistent trend was observed across all adsorbents: an increase in adsorbent dosage led to a corresponding enhancement in Cr(VI) removal efficiency. Specifically, the removal efficiency increased from 2 to 18.9% for CS, from 6 to 44.6% for CS/PVA, and from 80 to 98% for CS/PVA/GA as the dosage increased from 0.25 to 1 g. This improvement in removal efficiency can be attributed to the increase in the number of available active binding sites on the surface of the adsorbents with higher dosages, which promotes greater interaction between Cr(VI) ions and the composite material [39].

Among the tested materials, the CS/PVA/GA composite demonstrated the highest adsorption performance at all dosages, highlighting its superior affinity toward Cr(VI) ions due to its enhanced porosity, surface area, and chemical functionality. Based on the observed results, a dosage of 1 g was found to be optimal and was selected for subsequent experimental investigations.

Effect of Contact Time

The effect of contact time plays a crucial role in understanding the adsorption kinetics and determining the time required to reach equilibrium. In this study, the contact time was varied from 10 to 60 min to investigate its influence on Cr(VI) removal. The experiments were conducted at 30°C using an initial Cr(VI) concentration of 50 mg/l, adsorbent dose of 1 g in 30 ml solution, pH of 3 and stirring speed of 150 rpm. The results are depicted in Figure 9.

The data indicate that the removal efficiency increased progressively with contact time and eventually stabilized, reaching equilibrium at approximately 60 min. This behavior can be attributed to the abundance of active binding sites available on the adsorbent surface during the initial phase of contact. As time progressed, these sites gradually became saturated, leading to a plateau in adsorption capacity [40].

In the case of CS/PVA/GA, a more rapid and higher removal efficiency was observed compared to unmodified CS. This enhanced performance is likely due to the improved accessibility of functional groups and the increased number of active sites resulting from glutaraldehyde crosslinking. The initial rapid adsorption suggests that external surface adsorption plays a dominant role at the early stage, followed by slower intraparticle diffusion processes as the system approaches equilibrium.

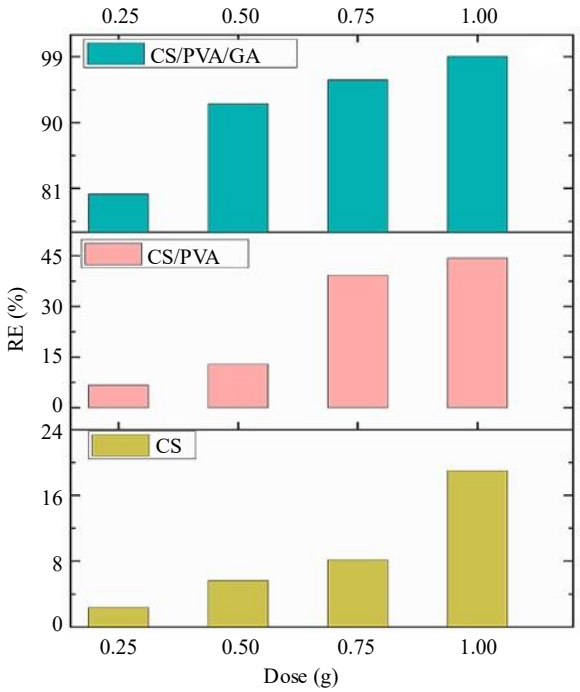

Figure 8. Effect of adsorbent dose on the adsorption of Cr(VI) on CS, CS/PVA and CS/PVA/GA composite.

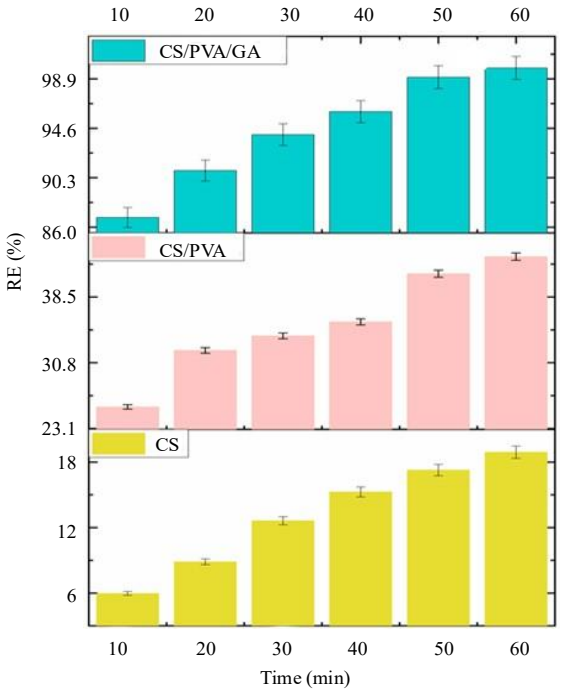

Figure 9. Effect of contact time on the adsorption of Cr(VI) on CS, CS/PVA and CS/PVA/GA composite.

The establishment of a 60-min equilibrium time provides valuable insight for optimizing contact duration in potential large-scale applications, ensuring both efficient metal ion removal and process feasibility.

Effect of initial concentration

The initial concentration of Cr(VI) plays a vital role in determining the adsorption behavior of the composite, as it influences the driving force for mass transfer between the aqueous phase and the adsorbent surface. To evaluate the effect of initial concentration, experiments were conducted over a concentration range of 25 to 150 mg/l at 30°C using an initial Cr(VI) concentration of 50 mg/l, pH of 3, stirring speed of 150 rpm, adsorbent dose of 1 g in 30 ml solution and a contact time of 60 min. The removal efficiencies for CS, CS/PVA, and CS/PVA/GA are presented in Figure 10.

The results showed that maximum Cr(VI) removal was observed at an initial concentration of 25 mg/l using CS, CS/PVA and CS/PVA/GA. At lower Cr(VI) concentrations (e.g., 25 mg/l), the removal efficiency was high across all adsorbents due to the availability of abundant active binding sites compared to the number of Cr(VI) ions. This resulted in stronger interactions between Cr(VI) and the functional groups (-NH_2, -OH) on the composite surface [17].

However, as the concentration increased beyond 100 mg/l, a gradual decline in removal efficiency was observed. This is likely due to the saturation of available binding sites and increased competition among Cr(VI) ions for adsorption, which limited the overall uptake capacity of the composites. The decline in removal efficiency at higher concentrations indicates that the adsorption system becomes less effective when overwhelmed by a high load of contaminants.

These findings are consistent with previous studies, which noted that Cr(VI) levels in industrial wastewater can frequently reach 50–100 mg/l, or higher [41]. Given Cr(VI) known toxicity, carcinogenicity, and environmental persistence, effective removal at such concentrations is essential. Consequently, further tests were conducted using 100 mg/l Cr(VI) to assess the practical applicability of the CS/PVA/GA composite in real-world wastewater treatment scenarios.

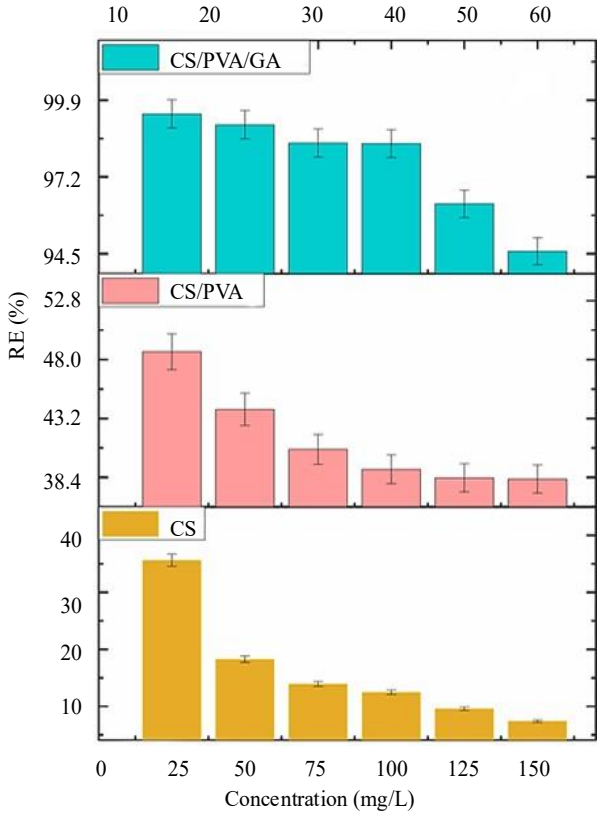

Figure 10. Effect of initial concentration of Cr(VI) on the adsorption of Cr(VI) on CS, CS/PVA and CS/PVA/GA composite.

Comparison of CS, CS/PVA, and CS/PVA/GA

The effect of different adsorbents unmodified chitosan (CS) and its modified composites (CS/PVA and CS/PVA/GA) on Cr(VI) removal efficiency and adsorption capacity was systematically evaluated at 30°C using initial Cr(VI) concentration of 100 mg/l, adsorbent dose of 1 g in 30 ml solution, pH of 3 and a constant stirring speed of 150 rpm. The findings are presented in Figure 10.

The results revealed a significant enhancement in Cr(VI) removal efficiency with the use of modified chitosan composites. Among the tested materials, CS/PVA/GA exhibited the highest removal efficiency of 98.9%, followed by CS/PVA at 44.3% and unmodified CS at 18.9%. These results highlight the superior performance of the covalently crosslinked CS/PVA/GA composite in comparison to unmodified or partially modified chitosan.

The marked improvement in the adsorption performance of CS/PVA/GA can be attributed to the introduction of glutaraldehyde (GA) as a covalent crosslinking agent. Crosslinking enhances the structural stability of the polymer network by preventing solubility in acidic conditions, a known limitation of unmodified CS due to its protonated amino groups. This increased stability promotes stronger binding interactions between the adsorbent and Cr(VI) ions, thereby boosting adsorption efficiency [42].

Moreover, the incorporation of GA introduces additional reactive sites and enhances the availability of functional groups (-NH_2 and -OH), which are critical for complexation with heavy metal ions. These findings are corroborated by FTIR data, which confirm significant interactions between Cr(VI) and the active functional groups, and by XRD analysis, which shows a predominantly amorphous structure in the CS/PVA/GA composite. The amorphous nature of the material is advantageous for adsorption processes due to its disordered structure and high accessibility of binding sites [43].

In conclusion, the results clearly demonstrate that the chemical modification of chitosan, especially via glutaraldehyde crosslinking, substantially improves the composite's adsorption capacity and makes CS/PVA/GA a highly efficient material for the removal of Cr(VI) from aqueous media.

Kinetic studies

The interaction of heavy metal ions with the surface of adsorbent materials can be comprehensively assessed through kinetic modeling. In this study, three kinetic models Pseudo-first order, Pseudo-second order, and Intraparticle diffusion were employed to interpret the adsorption behavior of Cr(VI) onto CS, CS/PVA, and CS/PVA/GA composites. The linearized forms of these models are given by Eqs. (3)–(5):

Pseudo-first order: $\ln(q_t - q_e) = lnq_{1\,(cal)} - k_1 t$ (3)

Pseudo-second order: $\frac{t}{q_t} = \frac{t}{q_{2\,(cal)}} + \frac{1}{k_2 q_{2(cal)}^2}$ (4)

Intraparticle diffusion: $q_t = k_{ID}\sqrt{t} + intercept$ (5)

where:

- q_t and q_e represent the amount of Cr(VI) adsorbed (mg/g) at time t and at equilibrium, respectively.
- k_1 and k_2 are the rate constants for the pseudo-first order and pseudo-second order models.
- $q_{1(cal)}$ and $q_{2(cal)}$ are the equilibrium adsorption capacities predicted by each model.
- K_{ID} is the intraparticle diffusion rate constant (mg/g·min$^{1/2}$).
- C is the intercept, which indicates the boundary layer effect.

The linear plots for all three kinetic models: ln q_e–q_t vs. t for pseudo-first-order, t/q_t vs. t for pseudo-second-order, and q_t vs. $t^{1/2}$ for intraparticle diffusion were analyzed to evaluate the adsorption kinetics, and the corresponding kinetic parameters along with correlation coefficients R^2 are summarized in Figure 11 and Table 2.

Among the tested models, the pseudo-second-order model best described the Cr(VI) adsorption kinetics for all adsorbents, as evidenced by the higher R^2 values. This suggests that chemisorption, involving valence forces through the sharing or exchange of electrons, is the predominant rate-limiting mechanism [44].

Furthermore, the intraparticle diffusion model exhibited a good fit, indicating the involvement of pore diffusion during the adsorption process [45]. However, since the q_t vs. $t^{1/2}$ plots did not pass through the origin, it implies that intraparticle diffusion was not the sole rate-limiting step.

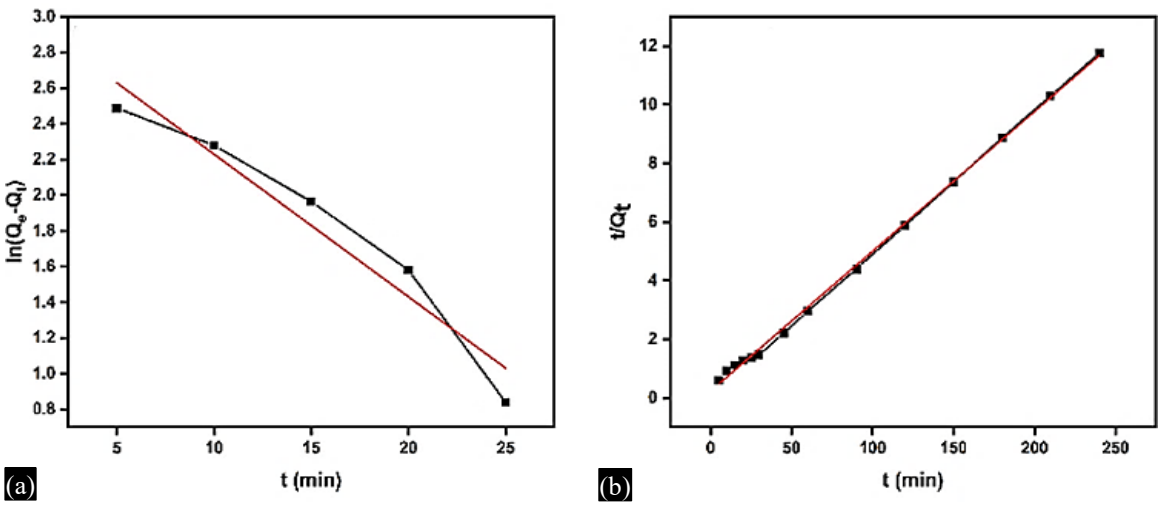

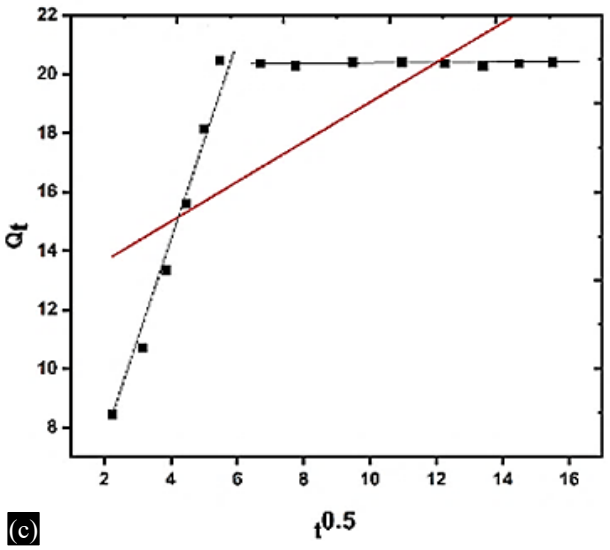

Figure 11. Adsorption kinetics of Cr (VI) using CS/PVA/GA composite modelled according to (a) Pseudo first order (b) Pseudo second order and (c) Intra-Particle Diffusion Model.

Table 2. Kinetic models for the uptake of Cr (VI) onto CS/PVA/GA composite.

Kinetic models	
Pseudo-first-order Model	
k_1 (l/min)	0.080
$q_{e,\,cal}$ (mg/g)	20.463
$q_{e,exp}$ (mg/g)	20.67
R^2	0.921
Pseudo-second-order Model	
k_2 (g/mg.min^{-1})	0.010
$q_{e,\,cal}$ (mg/g)	20.463
$q_{e,exp}$ (mg/g)	20.9741
R^2	0.998
Intra-particle diffusion Model	
K_{pi} (mg/g. min$^{1/2}$)	3.741
C	12.2920
R^2	0.980

The adsorption mechanism is thus controlled by both film diffusion and surface chemisorption. The successive steps in the adsorption process of Cr(VI) ions by CS/PVA/GA composite are understood to follow three primary mechanisms:

- *Film Diffusion:* Transport of Cr(VI) ions to the external surface of the adsorbent.
- *Pore Diffusion:* Migration of Cr(VI) ions through the pores of the adsorbent.
- *Surface Adsorption:* Attachment of Cr(VI) ions to the interior surface active sites.

Among these, the third step (adsorption on the surface) is considered rapid and is not typically rate-limiting. The rate-limiting step depends on the balance between film and pore diffusion:

- *Case I:* External diffusion > Internal diffusion → Rate governed by pore diffusion.
- *Case II:* External diffusion < Internal diffusion → Rate governed by film diffusion.
- *Case III:* External ≈ Internal diffusion → Formation of a boundary layer and gradual mass transfer.

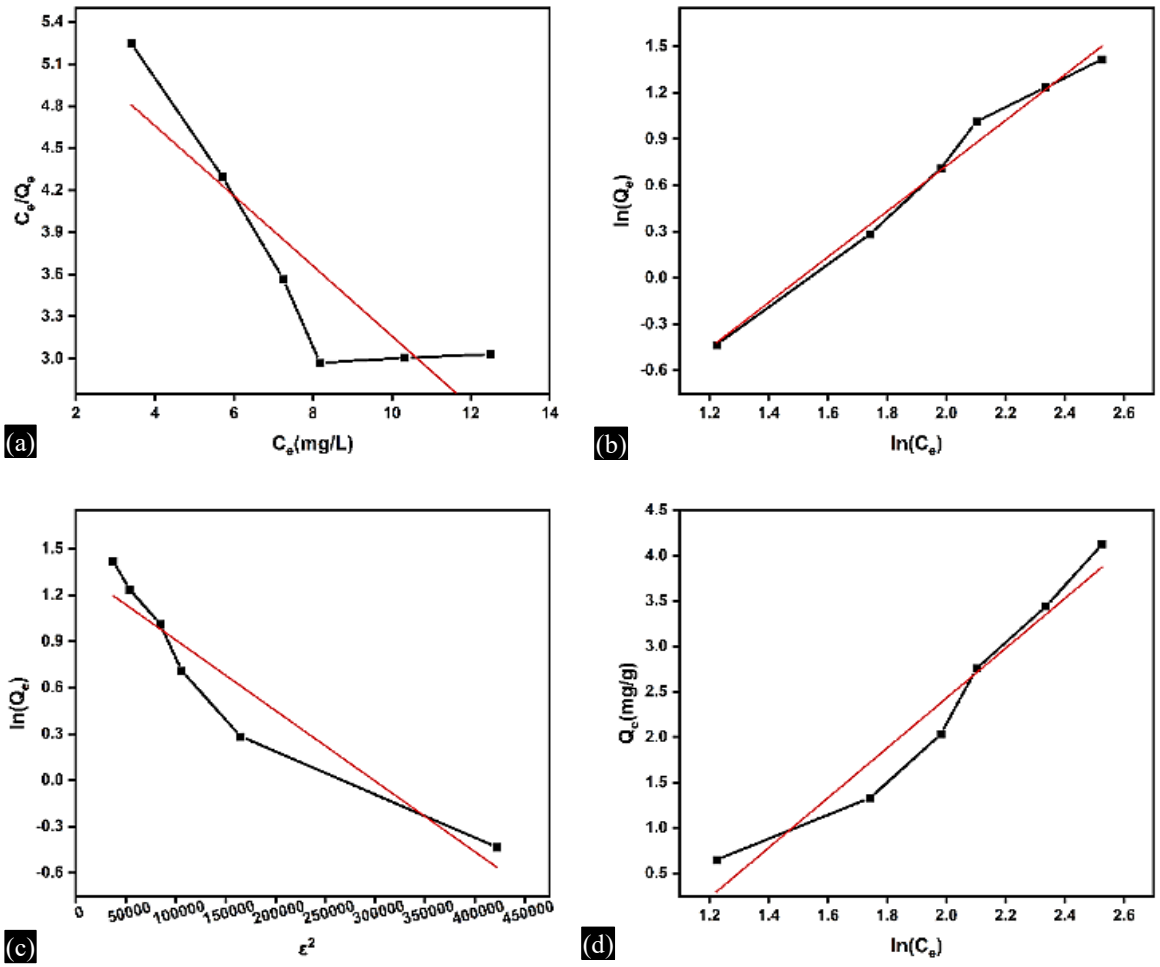

Figure 12. Modelling of adsorption by (a) Langmuir isotherm (b) Freundlich isotherm (c) Dubinin-Redushckevich isotherm model and (d) Temkin isotherm for CS/PVA/GA composite.

The enhanced adsorption kinetics observed for CS/PVA/GA can be attributed to the synergistic effect of PVA and glutaraldehyde (GA), which increase both the number of active sites and the accessibility of Cr(VI) ions to the adsorbent surface. Additionally, higher kinetic rate constants observed in this study compared to earlier reports indicate that Cr(VI) was adsorbed at high-energy, specific surface sites, underscoring the efficiency of the synthesized composite [46].

In conclusion, the kinetic data strongly support that the pseudo-second-order model governs the adsorption mechanism, confirming that physicochemical interactions, particularly chemisorption, play a dominant role in Cr(VI) uptake.

Isotherm Studies

To evaluate the nature of interactions between Cr(VI) ions and the CS/PVA/GA adsorbent, experimental data were analyzed using commonly employed adsorption isotherm models. These models provide insights into the adsorption mechanism, efficiency, and binding forces. The calculated isotherm constants and correlation coefficients R^2 are summarized in Table 3, while the linear plots of various isotherms fitted to the equilibrium data are presented in Figure 12.

Langmuir Isotherm

The Langmuir isotherm model assumes monolayer adsorption on a homogeneous surface with finite and identical binding sites, and no interaction between adsorbed molecules [47]. It is mathematically represented as:

Table 3. Isotherm parameters for the uptake of Cr (VI) onto CS/PVA/GA composite.

Isotherm models	
Langmuir Model	
q_m (mg/g)	0.1
K_L (l/mg)	0.3099
R_L	**0.0333**
R^2	0.984
Freundlich Model	
K_F mg.g^{-1} (mg/l)$^{-1/n}$	0.3802
1/n	0.677
R^2	0.988
Temkin Model	
A (l/g)	0.327527556
B (J/mol)	916.6
R^2	0.931
Doubinin-Radushkevich Model	
q_m (mg/g)	3.926
β (mol^2.kJ^{-2})	–0.0000046
E (kJ/mol)	330.4271191
R^2	**0.884**

$$q_e = \frac{q_{max} K_L C_e}{1 + K_L C_e} \tag{6}$$

The model implies that once an adsorbate occupies a site, no further adsorption can occur at that site. In this study, the separation factor (R_L) a dimensionless constant used to determine the favorability of adsorption was calculated using:

$$R_L = \frac{1}{1 + K_L C_O} \tag{7}$$

The calculated R_L value for CS/PVA/GA was 0.0333, indicating favorable adsorption ($0<R_L<1$). The Langmuir constant K_L was 0.3099 l/mg. While the Langmuir model describes the potential for monolayer formation, its correlation coefficient (R^2) was lower than that of the Freundlich model, suggesting a lesser fit to the experimental data.

Freundlich Isotherm

The Freundlich isotherm accounts for heterogeneous surface adsorption and assumes a multilayer formation with non-uniform heat of adsorption [48]. The model is expressed as:

$$q_e = K_F C_e^{1/n} \tag{8}$$

The model parameters include the Freundlich constant K_F and the intensity factor 1/n, where:

- $0<1/n<1$: Favorable adsorption,
- $1/n>1$: Unfavorable adsorption,
- $1/n=1$: Irreversible adsorption.

For CS/PVA/GA, the calculated value of 1/n=0.677, indicates favorable adsorption. The model also exhibited the highest correlation coefficient (R^2=0.988), signifying that the Freundlich isotherm provided the best fit to the experimental data, likely due to the heterogeneous surface of the composite.

Temkin Isotherm

The Temkin isotherm assumes that the heat of adsorption of all molecules in the layer decreases linearly with coverage due to adsorbate–adsorbate interactions. Although this model is more accurate

for gas-phase adsorption, it is often used in liquid-phase studies [49]. However, for complex aqueous systems like biosorption of heavy metals, Temkin's assumptions are often oversimplified. The presence of solvent interactions, micelle formation, and various solvation effects make the liquid-phase adsorption more complex.

In this study, the Temkin model exhibited a reasonable correlation coefficient (R^2>0.931), indicating a moderate fit, though not as strong as Freundlich.

Dubinin Radushkevich (D–R) Isotherm

The Dubinin-Radushkevich (D-R) isotherm model is typically used to distinguish between physical and chemical adsorption by estimating the mean free energy of adsorption [50]. Although not the best-fitting model in this study, the D-R model still showed a high correlation coefficient, suggesting that chemisorption may play a dominant role in the Cr(VI) adsorption process on CS/PVA/GA composite.

The strong correlation of experimental data with the Freundlich model and the evidence of pore diffusion (from kinetic analysis) suggests that adsorption occurs on a heterogeneous surface and is governed by both surface chemisorption and internal diffusion mechanisms.

Desorption experiments

The adsorption-desorption experiments were performed to assess the reusability and regeneration potential of the CS/PVA/GA composite [51]. The initial adsorption (Cycle 0) was conducted under optimal conditions: initial Cr(VI) concentration of 100 mg/l, pH 3, temperature 30°C, and adsorbent dose of 1 g in 30 ml of solution. After the initial adsorption, the Cr(VI)-loaded CS/PVA/GA beads were thoroughly rinsed with distilled water to eliminate unbound Cr(VI) and subsequently oven-dried at 40°C.

To regenerate the adsorbent, the dried Cr(VI)-loaded beads were immersed in 30 ml of desorbing agents either 0.1 M NaOH, and soaked for 2 h. Following desorption, the beads were repeatedly washed with distilled water until neutral pH was achieved and then dried again at 40°C. The regenerated adsorbent was then used for the next adsorption cycle under identical experimental conditions. This cyclic process was continued until a significant decline in Cr(VI) adsorption efficiency was observed. The desorption results are presented in Figure 13.

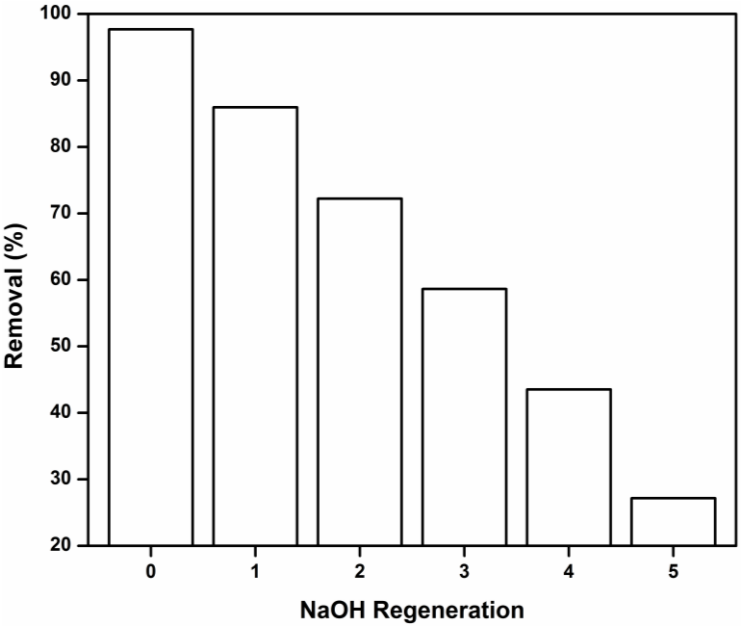

Figure 13. Regeneration study of CS/PVA/GLA composite.

The desorption efficiency (D%) after each cycle was evaluated using the following equation:

$$D\% = {}^{m_{des}}/_{m_{ads}} * 100 \quad (9)$$

where:

- m_{ads} is the amount of Cr(VI) adsorbed (mg),
- m_{des} is the amount of Cr(VI) desorbed (mg).

These quantities were calculated using:

$$m_{des}=C_e \times V^1 \text{ and } m_{ads}=(C_o - C_e) \times V \quad (10)$$

where:

- C_o and C_e are the initial and equilibrium concentrations of Cr(VI) (mg/l), respectively,
- V is the volume of the Cr(VI) solution used during adsorption (l),
- V^1 is the volume of the desorbing solution (l).

UV-Vis spectrophotometry was employed to monitor Cr(VI) concentrations after each adsorption and desorption cycle. The desorption performance and adsorption retention over successive cycles offer insight into the economic viability and sustainability of the CS/PVA/GA composite as a regenerable biosorbent.

CONCLUSION

In this study, a novel CS/PVA/GA composite adsorbent was successfully synthesized through the crosslinking of chitosan and polyvinyl alcohol using glutaraldehyde, with the goal of enhancing Cr(VI) removal from aqueous solutions. Comprehensive characterization using FESEM-EDS, XRD, BET, and FTIR confirmed the structural integrity, surface morphology, porosity, and functional groups essential for effective adsorption. Batch adsorption experiments demonstrated that the composite exhibited significantly improved adsorption performance, achieving a high maximum adsorption capacity of 98.9 mg/g.

Kinetic analysis revealed that the adsorption process follows a pseudo-second-order model, indicating chemisorption as the dominant mechanism. The equilibrium data fit best with the Freundlich isotherm model, suggesting a heterogeneous adsorption surface.

Notably, the CS/PVA/GA composite maintained a high level of performance after multiple reuse cycles, with a desorption efficiency of 73% after three cycles, highlighting its stability and reusability. These findings demonstrate that the chemically modified chitosan-based composite is a promising, sustainable, and cost-effective material for the removal of toxic Cr(VI) from wastewater, making it a strong candidate for practical environmental remediation applications.

REFERENCES

1. Barnhart J. Occurrences, uses, and properties of chromium. Reg Toxic Pharm. 1997; 26(1 Pt 2): 3–7.
2. US Environmental Protection Agency (USEP). Quality criteria for water. EPA Publication 440/5-86-001, U.S. Gov. Printing Office, Washington D.C. 1987.
3. World Health Organization (WHO). Guidelines for drinking-water quality. 2004.
4. Demirbas A. Heavy metal adsorption onto agro-based waste materials: A review. J Hazard Mater. 2008; 157(2–3): 220–229.
5. Golder AK, Chanda AK, Samanta AN, Ray S. Removal of Cr(VI) from aqueous solution: Electrocoagulation vs chemical coagulation. Sep Sci Technol. 2007; 42(10): 2177–2193.
6. Ba S, Alagui A, Hajjaji M. Retention and release of hexavalent and trivalent chromium by chitosan, olive stone activated carbon, and their blend. Environ Sci Pollut Res Int. 2018; 25(20): 19585–19604.

7. Beheshti H, Irani M, Hosseini L, Rahimi A, Aliabadi M. Removal of Cr (VI) from aqueous solutions using chitosan/MWCNT/Fe_3O_4 composite nanofibers-batch and column studies. Chem Eng J. 2016; 284: 557–564.
8. Chopra H, *et al*. Preparation and evaluation of chitosan/PVA based hydrogel films loaded with honey for wound healing application. Gels. 2022; 8(2): 111.
9. Gonenc I, Us F. Effect of glutaraldehyde crosslinking on degree of substitution, thermal, structural, and physicochemical properties of corn starch. Starch-Stärke. 2019; 71(3–4): 1800046.
10. Perez-Calderon J, Marin-Silva DA, Zaritzky N, Pinotti A. Eco-friendly PVA-chitosan adsorbent films for the removal of azo dye Acid Orange 7: Physical cross-linking, adsorption process, and reuse of the material. Adv Ind Eng Polym Res. 2023; 6(3): 239–254.
11. Song Q, Gao J, Lin Y, Zhang Z. Synthesis of cross-linking chitosan-PVA composite hydrogel and adsorption of Cu(II) ions. Water Sci Technol. 2020; 81(5): 1063–1070.
12. Altun T, Ecevit H. Cr(VI) removal using Fe_2O_3-chitosan cherry kernel shell pyrolytic charcoal composite beads. Environ Eng Res. 2019; 25(3): 426–438.
13. Zhang S, *et al*. Malic acid-enhanced chitosan hydrogel beads (mCHBs) for the removal of Cr(VI) and Cu(II) from aqueous solution. Chem Eng J. 2018; 353: 225–236.
14. Du X, Kishima C, Zhang H, Miyamoto N, Kano N. Removal of Chromium(VI) by Chitosan Beads Modified with Sodium Dodecyl Sulfate (SDS). Appl Sci. 2020; 10(14): 4745.
15. Chauhan D, Jaiswal M, *et al*. Removal of cadmium and hexavalent chromium from electroplating wastewater using thiocarbamoyl chitosan. Carbohydr Polym. 2012; 88(2): 670–675.
16. Eladlani N, Dahmane EM, Ouahrouch A, Rhazi M, Taourirte M. Recovery of Chromium(III) from Tannery Wastewater by Nanoparticles and Whiskers of Chitosan. J Polym Env. 2018; 26: 152–157.
17. Popescu I, *et al*. Eco-friendly synthesized PVA/chitosan/oxalic acid nanocomposite hydrogels embedding silver nanoparticles as antibacterial materials. Gels. 2022; 8(5): 268.
18. Eldeeb TM, El Nemr A, Khedr MH, El-Dek SI, Imam NG. Novel three-dimensional chitosan-carbon nanotube–PVA nanocomposite hydrogel for removal of Cr(VI) from wastewater. Desalin Water Treat. 2020; 184: 163–177.
19. Mahmoodi NM, Mokhtari-Shourijeh Z. Preparation of PVA-chitosan blend nanofiber and its dye removal ability from colored wastewater. Fibers Polym. 2015;16:1861–1869. doi: 10.1007/s12221-015-5371-1.
20. Nowruzi R, Heydari M, Javanbakht V. Synthesis of a chitosan/polyvinyl alcohol/activate carbon biocomposite for removal of hexavalent chromium from aqueous solution. Int J Biol Macromol. 2020; 147: 209–216.
21. Sugashini S, Gopalakrishnan S. Studies on the performance of protonated cross-linked chitosan beads (PCCB) for chromium removal. Res J Chem Sci. 2012; 2(6): 55–59.
22. Eliodório KP, Pereira GJ, de Araújo Morandim-Giannetti A. Functionalized chitosan with butylammonium ionic liquids for removal of Cr(VI) from aqueous solution. J Appl Polym Sci. 2021;138(9):49912. doi: 10.1002/app.49912.
23. Emamy FH, Bumajdad A, Lukaszewicz JP. Adsorption of hexavalent chromium and divalent lead ions on the nitrogen-enriched chitosan-based activated carbon. Nanomaterials. 2021; 11(8): 1907.
24. Hadi Najafabadi H, Irani M, Roshanfekr Rad L, Heydari Haratameh A, Haririan I. Removal of Cu^{2+}, Pb^{2+} and Cr^{6+} from aqueous solutions using a chitosan/graphene oxide composite nanofibrous adsorbent. RSC Adv. 2015; 5(21): 16532–16539.
25. Huang G, Zhang H, Shi JX, Langrish TAG. Adsorption of chromium(VI) from aqueous solutions using cross-linked magnetic chitosan beads. Ind Eng Chem Res. 2009; 48(5): 2646–2651.
26. Subedi N, *et al*. A comparative study of magnetic chitosan (Chi@Fe3O4) and graphene oxide modified magnetic chitosan (Chi@Fe3O4GO) nanocomposites for efficient removal of Cr(VI) from water. Int J Biol Macromol. 2019; 137: 948–959.
27. Krishna Kumar AS, Jiang SJ, Tseng WL. Effective adsorption of chromium(VI)/Cr(III) from aqueous solution using ionic liquid functionalized multiwalled carbon nanotubes as a super sorbent. J Mater Chem A. 2015; 3(13): 7044–7057.
28. Kumari S, Rath P, Kumar ASH, Tiwari TN. Removal of hexavalent chromium using chitosan prepared from shrimp shells. Afr J Biotechnol. 2016; 15(3): 50–54.

29. Huang Y, *et al*. Fast and efficient removal of chromium (VI) anionic species by a reusable chitosan-modified multi-walled carbon nanotube composite. Chem Eng J. 2018; 339: 259–267.
30. Jorge Gonçalves F, *et al*. Application of pyridine-modified chitosan derivative for simultaneous adsorption of Cu(II) and oxyanions of Cr(VI) from aqueous solution. J Environ Manage. 2021; 282: 111939.
31. Kaur R, Goyal D, Agnihotri S. Chitosan/PVA silver nanocomposite for butachlor removal: Fabrication, characterization, adsorption mechanism and isotherms. Carbohydr Polym. 2021; 262: 117906.
32. Marques Neto JdeO, Bellato CR, Silva DdeC. Iron oxide/carbon nanotubes/chitosan magnetic composite film for chromium species removal. Chemosphere. 2019; 218: 391–401.
33. Lei C, Wang C, Chen W, He M, Huang B. Polyaniline@magnetic chitosan nanomaterials for highly efficient simultaneous adsorption and in-situ chemical reduction of hexavalent chromium: Removal efficacy and mechanisms. Sci Total Environ. 2020; 733: 139316.
34. Rathinam K, Singh SP, Arnusch CJ, Kasher R. An environmentally friendly chitosan-lysozyme biocomposite for the effective removal of dyes and heavy metals from aqueous solutions. Carbohydr Polym. 2018; 199: 506–515.
35. Li L, *et al*. Biomaterials cross-linked graphene oxide composite aerogel with a macro–nanoporous network structure for efficient Cr (VI) removal. Int J Biol Macromol. 2020; 156: 1337–1346.
36. Peligro FR, Pavlovic I, Rojas R, Barriga C. Removal of heavy metals from simulated wastewater by in situ formation of layered double hydroxides. Chem Eng J. 2016; 306: 1035–1040.
37. Hossain KFB, Sikder MT, Rahman MM, Uddin MK, Kurasaki M. Investigation of chromium removal efficiency from tannery effluent by synthesized chitosan from crab shell. Arab J Sci Eng. 2017; 42: 1569–1577.
38. Chen D, Yang K, Wang H, Zhou J, Zhang H. Cr(VI) removal by combined redox reactions and adsorption using pectin-stabilized nanoscale zero-valent iron for simulated chromium contaminated water. RSC Adv. 2015; 5(80): 65068–65073.
39. Sarfraz S, *et al*. Removal of hexavalent chromium ions using micellar modified adsorbent: isothermal and kinetic investigations. RSC Adv. 2022; 12(37): 23898–23911.
40. Nithya R, Sudha PN. Removal of heavy metals from tannery effluent using chitosan-g-poly(butyl acrylate)/bentonite nanocomposite as an adsorbent. Text Cloth Sustain. 2017; 2(1): 7.
41. Cheung WH, Szeto YS, McKay G. Intraparticle diffusion processes during acid dye adsorption onto chitosan. Bioresour Technol. 2007; 98(15): 2897–2904.
42. Thinh NN, *et al.* Magnetic chitosan nanoparticles for removal of Cr(VI) from aqueous solution. Mater Sci Eng C Mater Biol Appl. 2013; 33(3): 1214–1218.
43. Wang X, *et al*. Triethylenetetramine-modified hollow Fe_3O_4/SiO_2/chitosan magnetic nanocomposites for removal of Cr(VI) ions with high adsorption capacity and rapid rate. Microporous Mesoporous Mater. 2020; 297: 110041.
44. Habiba U, Afifi AM, Salleh A, Ang BC. Chitosan/(polyvinyl alcohol)/zeolite electrospun composite nanofibrous membrane for adsorption of Cr^{6+}, Fe^{3+} and Ni^{2+}. J Hazard Mater. 2017; 322(Pt A): 182–194.
45. Pholosi A, Naidoo EB, Ofomaja AE. Intraparticle diffusion of Cr(VI) through biomass and magnetite coated biomass: A comparative kinetic and diffusion study. South Afr J Chem Eng. 2020; 32: 39–55.
46. Iqbal J, *et al*. Adsorption of acid yellow dye on flakes of chitosan prepared from fishery wastes. Arab J Chem. 2011; 4(4): 389–395.
47. Villarante N, Bautista APR, Sumalapao DEP. Batch adsorption study and kinetic profile of Cr(VI) using Lumbang (Aleurites moluccana)-derived activated carbon-chitosan composite crosslinked with epichlorohydrin. Orient J Chem. 2017; 33: 1111–1119.
48. Labied R, Benturki O, Hamitouche AYE, Donnot A. Adsorption of hexavalent chromium by activated carbon obtained from a waste lignocellulosic material (Ziziphus jujuba cores): Kinetic, equilibrium, and thermodynamic study. Adsorpt Sci Technol. 2018; 36(3–4): 1066–1099.

49. Owalude SO, Tella AC. Removal of hexavalent chromium from aqueous solutions by adsorption on modified groundnut hull. Beni-Suef Univ J Basic Appl Sci. 2016; 5(4): 377–388.
50. Samuel M, Bhattacharya J, Raj S, Santhanam N, Singh H, Pradeep Singh ND. Efficient removal of Chromium(VI) from aqueous solution using chitosan grafted graphene oxide (CS-GO) nanocomposite. Int J Biol Macromol. 2019; 121: 285–292.
51. Vilela PB, *et al*. Adsorption and removal of chromium (VI) contained in aqueous solutions using a chitosan-based hydrogel. Environ Sci Pollut Res Int. 2019; 26(28): 28481–28489.

